

Adeno-associated virus perfusion enhanced expression: A commercially scalable, high titer, high quality producer cell line process

Wei Xue,¹ Cameron Fulco,^{1,2} Sha Sha,¹ Nick Alden,¹ Jan Panteli,¹ Patrick Hossler,¹ and James Warren¹

¹Ultragenyx Pharmaceutical Inc., Global CMC Development, 19 Presidential Way, Woburn, MA 01801, USA

With safety and efficacy demonstrated over hundreds of clinical trials in the last 30 years, along with at least six recent global marketing authorizations achieved since 2017, recombinant adeno-associated viruses (rAAVs) have been established as the leading therapeutic gene transfer vector for rare, monogenic diseases. Significant advances in manufacturing technology have been made in the last few decades to address challenges with GMP production of rAAV products, although yield, cost, scalability, and quality remain a challenge. With transient transfection processes established as a manufacturing platform for multiple commercial AAV products, there remains significant yield, cost, robustness, and scalability constraints that need to be resolved to enable a reliable supply of rAAV products for global patient access. The development of stable producer cell lines for rAAV products has enabled scalability and, in some cases, improvements in productivity. Herein we describe a novel AAV perfusion-enhanced expression (APEX) process, resulting in higher maximum cell densities in the production bioreactor with a 3- to 6-fold increase in volumetric productivity. This process has been successfully demonstrated across multiple serotypes in large scale cell culture with titers approaching 1×10^{12} GC/mL. The APEX production platform marks a significant leap forward in the efficient and effective manufacturing of rAAV vector products.

INTRODUCTION

Recombinant adeno-associated viruses (rAAV) have been evaluated as therapeutic gene transfer vectors since the late 1990s, initially explored as vectors to deliver the human CFTR gene to treat cystic fibrosis.¹ Several attributes make rAAV vectors highly attractive as clinical gene transfer vector candidates: AAV is nonpathogenic in humans, able to infect dividing as well as nondividing cells, and can be selected or engineered for the desired tissue-specific tropism with high transduction efficiency.^{2,3}

By the turn of the century, advancement in manufacturing technology sufficient to generate higher concentrations of purified clinical grade rAAV product was key in establishing AAVs as potentially the most effective and safe vector systems for therapeutic gene transfer clinical development.⁴ Early AAV vector packaging systems utilized adherent HEK-293 with a three-plasmid transfection system, including a

plasmid providing the therapeutic gene sequence flanked by AAV2 ITRs,⁵ a second plasmid containing AAV *rep* and *cap* genes, and a third plasmid containing helper elements required for replication (E2A, E4orf6, VA), while the HEK-293 cell line provided additional required helper elements E1A and E1B. As the need for a greater volume of clinical AAV vector arose, the plasmid transfection process was readily transitioned to a HEK-293 suspension system. Manufacturing rAAV products in a stirred-tank bioreactor system using serum-free medium and optimized transfection reagents such as polyethyleneimine enabled industrial scale production. Recently, proof of concept for operating this platform with an intensified, perfusion-based feeding strategy has been established.⁶ While the HEK-293 system has been successfully scaled to 1000L or higher, the cost of plasmids (especially Good Manufacturing Process [GMP]-grade plasmids) is still considerable. In addition, the plasmid-transfection reagent complex must be carefully managed through precise volume ratios, mixing conditions, time, and temperature. Significant fluid-dynamic challenges exist at industrial scale, which present a risk to the large-scale transfection process, further challenging the consistent and robust manufacture of high-yielding bioprocesses.

While large-scale transient transfection processes present numerous financial and engineering challenges, the use of stable, scalable producer cell lines (PCLs) provides an alternative manufacturing approach that is closer to industrial processes used to manufacture protein biologics at high volume and yield. The development of a stable PCL for AAV packaging was first described almost 30 years ago, using a HeLa cell parental substrate with integrated AAV Rep and Cap elements which were induced by adenovirus 5 (Ad5) infection.⁷ This system was subsequently scaled for clinical manufacturing of AAV gene therapy vectors and demonstrated to be highly scalable.^{8,9} In the Pinnacle PCL platform, HeLa S3 cells are stably integrated with inducible *Rep* genes, *Cap* genes, and inverted terminal repeat-flanked

Received 19 December 2023; accepted 10 May 2024;
<https://doi.org/10.1016/j.omtm.2024.101266>.

²Present address: AbbVie Inc., 100 Research Dr, Worcester, MA 01605, USA

Correspondence: James Warren, Ultragenyx Pharmaceuticals, 19 Presidential Way, Woburn, MA 01801, USA.

E-mail: jwarren@ultragenyx.com



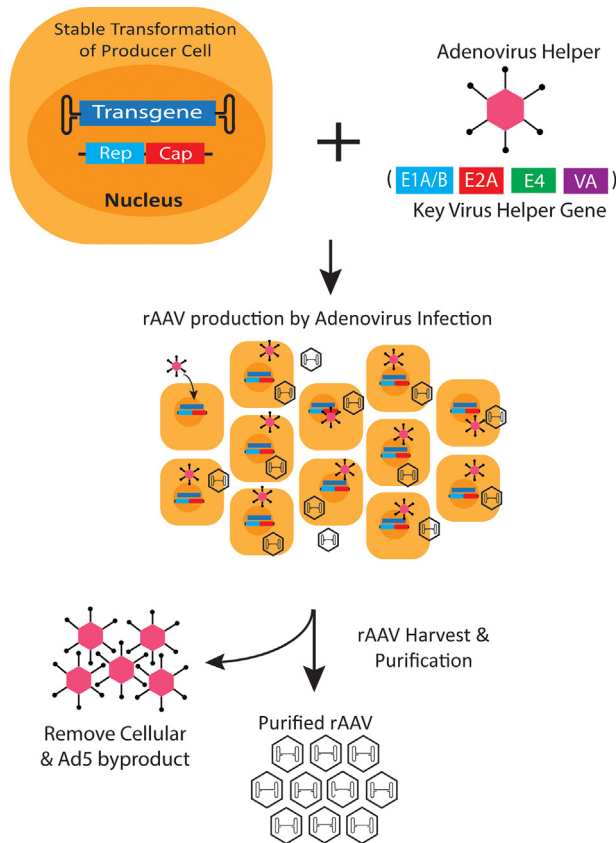


Figure 1. AAV/helper virus Pinnacle PCL platform

The Pinnacle PCL platform incorporates the AAV Rep/Cap and transgene, flanked by inverted terminal repeat (ITR) sequences stably integrated into the production cell genome. AAV production is performed in serum-free suspension culture through the addition of a helper virus (adenovirus) to initiate AAV replication in the bioreactor (only key genes for AAV production shown in the figure). Subsequent downstream purification works to remove impurities, cellular and helper-virus by-products, and concentrate purified AAV particles.

transgene using a triple play plasmid transfection. Production of rAAV is triggered by introducing wild-type Ad5 to provide helper elements E1A/B, E2A and E4/Orf6, and VA RNA (Figure 1). This platform presents several advantages compared with HEK-293. First, as the transgenes, *Rep* genes and *Cap* genes are stably transfected in the cells, rAAV production and packaging are significantly more robust, yielding higher full capsid percentage (approximately 40%–80% of PCL vs. 5%–10% with HEK-293 from bulk harvest material by affinity capture without enrichment, in house data). Second, the Ad5 infection is a fast and robust process, with E1A gene expressed as early as 2 h post infection (hpi).¹⁰ The Ad5 infection is more scalable compared with a transfection-based process, as Ad5 is significantly more stable over time than its counterpart transfection complex. Third, the wild-type Ad5 can be readily produced with infection of Ad5 into wild-type HeLa S3 cells to establish GMP viral banks, which is significantly more cost effective than GMP-grade plasmid. Routine and well-characterized downstream viral clearance unit operations such as heat inacti-

vation, viral filtration, and ion exchange filtration/chromatography mitigate the concern of Ad5 clearance.

Although the PCL-based process demonstrated several GMP-friendly traits, improving the low yield of rAAV and high manufacturing cost of production remains essential for global patient access. In the batch production mode, maintaining a cell culture beyond a very low upper cell density limit (1.5×10^6 viable cells/mL), proves counterproductive for rAAV yield (i.e., cell density effect). In this work, we developed the AAV Perfusion-Enhanced Expression (APEX) process, which is scalable and high yielding ($\leq 1 \times 10^{12}$ GC/mL). By elucidating by-product accumulation as the key facilitating factor of the cell density effect in the rAAV production, perfusion was chosen to modify the batch process to support higher cell density without sacrificing cell specific productivity (qP). This approach was further optimized, characterized, and proven scalable up to 250L scale. Through significant upstream yield improvements mediated through APEX, reduction in cost of production is anticipated, with the potential to greatly expand global patient access to gene therapy products.

RESULTS

Cell density effect observed in rAAV batch PCL production system

The cell density effect describes the historical observation of an indirect relationship between viable cell density (VCD) and rAAV titers.¹¹ To further map the existence of the cell density effect in our PCL platform, three infection VCDs ranging from 1.3×10^6 to 5.2×10^6 viable cells/mL (vc/mL) were tested in batch mode in an Ambr15 production vessel with no change to the other operating conditions, such as temperature, pH and multiplicity of infection (MOI). The higher VCD at the time of infection (Figure 2A) led to faster glucose consumption and lactate production (Figure 2B). Moderate increases in infection VCD resulted in a disproportionate log reduction in rAAV harvest titer (10-fold, Figure 2C) and cell qP (100-fold) (Figure 2D). The results agreed with the cell density effect observed in other biologics production systems.¹¹ The root cause of the cell density effect has not been well characterized for AAV production systems.

Nutrient deficiency is not the cause of cell density effect

One hypothesis for the cause of the cell density effect is the potential for nutrient deficiency in batch mode. To evaluate this hypothesis, spent media analysis was conducted. Daily spent media samples from seven batch cultures of a PCL expressing an AAVhu37 product at a 3L scale were tested for amino acid levels after Ad5 infection. The concentrations were normalized to that at the time of infection (day 0), with accumulation shown in green and consumption in red (Figure 3A). Cystine was below the limit of quantification in all samples and hence not listed. Only glucose and glutamine showed significant consumption over the course of batch mode rAAV production, which was expected. Alanine, glutamate, glycine, and proline accumulated throughout the culture duration.

With glucose and glutamine identified as media components with the highest consumption rates, a feed study was performed to evaluate

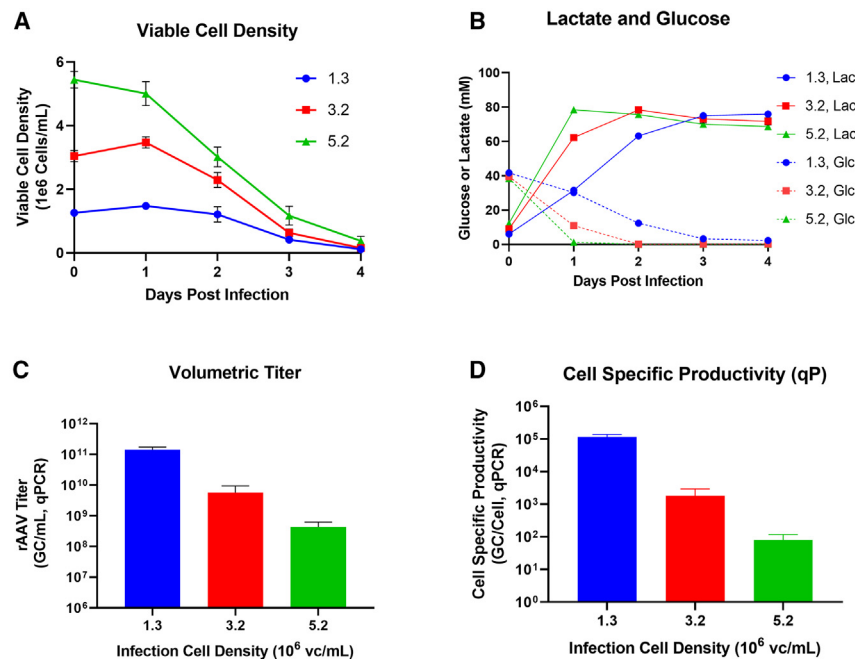


Figure 2. Cell density effect observed in rAAV production demonstrated at 1.3×10^6 vc/mL (blue), 3.2×10^6 vc/mL (red) and 5.2×10^6 (green) vc/mL infection VCD

(A) VCD time profile. (B) Glucose (dash) and lactate (solid) time profile. (C) Volumetric titer. (D) Cell qP. Data are presented as mean \pm SD.

whether media component additions would recover rAAV titers. In batch mode, we evaluated an infection VCD of 1.2×10^6 vc/mL (control), 1.8×10^6 vc/mL, and 1.8×10^6 vc/mL with additional daily feeds of glucose and glutamine to restore these nutrients back to fresh media levels. In these fed-batch cultures, we observed that glucose consumption rate remained lower than the control (Figure 3B), glutamine consumption rate recovered to the level of control (Figure 3C), and cell-specific rAAV productivity (qP) was the lowest of all conditions tested (Figure 3D). These results suggest that nutrient deficiency is not the cause of the cell density effect in our PCL platform.

Metabolic waste products promote the cell density effect

To test if metabolic waste products actively inhibited rAAV production, sodium lactate and ammonium chloride were added into batch production conditions at concentrations ranging from 0 to 30 mM and 0 to 3 mM, respectively, prior to infection. The contour plot (Figure 4A) shows the impact that lactate and ammonium have on lowering rAAV production. Harvest yield decreased when increasing the concentration of either metabolite with the largest decrease being the combination of 30 mM sodium lactate and 3 mM ammonium.

To reduce waste metabolite accumulation, approaches to modulate metabolism and reduce their production were explored. To reduce lactate production, cell culture pH setpoint was reduced from 7.8 to 7.4 at VCDs of 1.3×10^6 vc/mL (control) and 2.6×10^6 vc/mL. Lactate accumulation was reduced with lower pH at both levels of VCDs (Figure 4B) through lowering the lactate production rate (Figure 4C), but only mildly improved the qP (Figure 4D). Because glutamine hydrolysis to glutamate and ammonium was the most substantial source of ammonium accumulation in this cell culture process, we hypothesized that substituting glutamine with

the L-alanyl-L-glutamine (glutamax) dipeptide would mitigate the accumulation of toxic ammonium by-product. In the next study, L-alanyl-L-glutamine dipeptide was supplemented to the production media ranging from 6 mM to 10 mM, instead of 6 mM glutamine. Although ammonium accumulation levels were reduced (Figure 4E) through less cell-specific ammonium production rate (Figure 4F), the rAAV cell qP was reduced at all levels tested (Figure 4G).

After observing high metabolite accumulation and low metabolite production rates as both detrimental to rAAV production, we hypothesized that a bioprocessing approach that precludes lactate/ammonium accumulation, while simultaneously maintaining their production rates, would be supportive of higher rAAV production. An abbreviated perfusion mode was developed to support high cell density and low lactate/ammonium accumulation, without sacrificing cell qP.

APEX process overview

The APEX process platform leverages perfusion during the production bioreactor to support a higher cell density that maintains cell qP relative to a lower cell density batch culture, summarized in Table 1. The production parameters are discussed in the following sections.

Characterization and optimization of the APEX process

Initial perfusion rate and timing establishment

During the initial development of the APEX process (referred as APEX P1), we leveraged data obtained in the batch production to establish the version of APEX process. The perfusion period post infection was determined through rAAV kinetics observed in batch mode. The cell retention device in the perfusion system utilizes a hollow fiber filter with a 0.2- μ m nominal pore size, which allows free passage of both Ad5 and AAV. Hence, after the infection, the perfusion should not restart until sufficient time for Ad5 binding and internalization to the production cells and should stop before the rAAV is released from the cells. Crisostomo and colleagues¹⁰ demonstrated that the earliest gene transcripts (e.g., E1A) are detectable as soon as 2 hpi. Since only rAAV in the bioreactor supernatant will be passed along to the downstream process to subsequently generate drug substance, a high percentage of extracellular rAAV is desired. The percentage of extracellular rAAV is calculated by comparing the titer

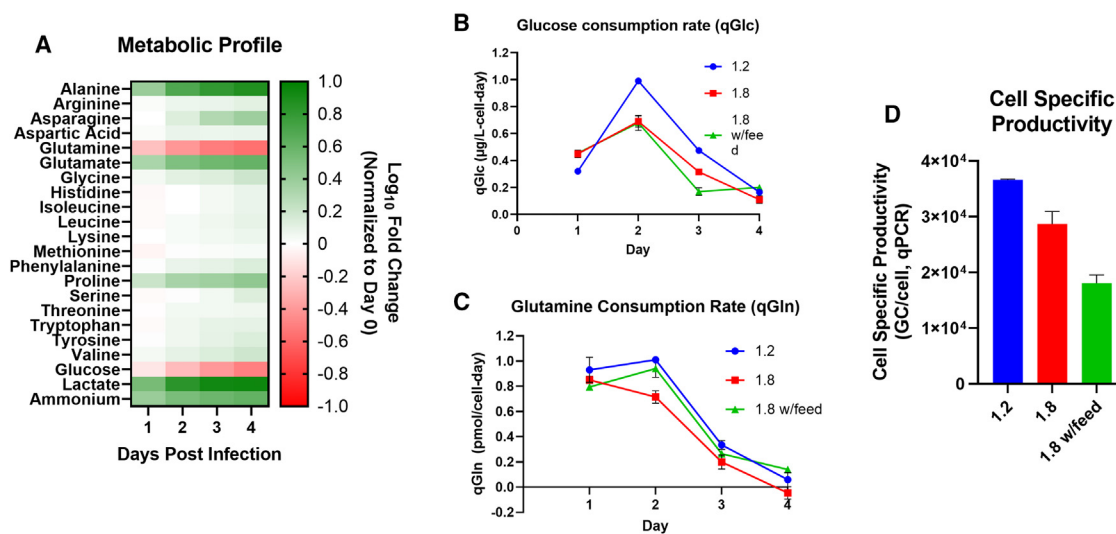


Figure 3. Nutrient deficiency is not the cause for cell density effect

Normalized metabolic profile post infection are shown in (A). Batch process with infection VCD of 1.2×10^6 vc/mL (blue), 1.8×10^6 vc/mL (red), and 1.8×10^6 vc/mL with glucose and glutamine daily feed (green) were compared in (B) glucose consumption rate, (C) glutamine consumption rate, and (D) Cell qP. Data are shown represent $n = 2$ (where relevant) and presented as mean \pm SD.

results from cell culture supernatant and culture suspension treated with the detergent Triton X-100, which lyses cells, and it trends closely with dead cell percentage (Figure 5A). Observing less than 3% rAAV released on day 2, the perfusion stop time was selected as 48 hpi.

A metabolic model (detailed in the Materials and methods section) was created with batch process data including nutrient consumption rate and waste production rate. The purpose of the model is to predict the metabolic profiles dependency on different perfusion schemes in the APEX process, hence allowing the rational selection of process parameters to avoid unfavorable waste by-product accumulation. When assuming a manageable 2.5 vessel volume per day (VVD) during 2–48 hpi, the model predicted a sufficiently low lactate and ammonium level (up to approximately 2.5 g/L and 2.5 mM, respectively) to avoid a cell density effect. We verified the results first with AAVhu37 serotype, demonstrating that VCD, glucose, lactate, glutamine, and ammonium using APEX process were comparable to the model predictions (demonstrated in Figures 5B and 5C) (overall $R^2 = 0.98$). In addition, further laboratory-scale experiments showed a 3- to 4-fold increase in harvest yield in additional serotypes including AAV9 and AAV8 (Figure 5D). The cell qP improvement through APEX is thus serotype agnostic within clades E (hu37 and AAV8) and F (AAV9). Since both titer and cell density were directly correlated, it was demonstrated that the cell density effect was eliminated by the APEX process.

Product quality attributes of exemplar batch process and APEX process were compared and are summarized in Table S1. We observed elevated levels of impurities, including host-cell DNA, host-cell protein, and Ad5 DNA in the bulk harvest of APEX process, which are

expected due to the higher cell mass. We observed similar and acceptable levels of each impurity after purification step designed to remove it (e.g., host cell DNA removal by anion-exchange chromatography). We considered the potency equivalent between the drug substance of the two processes, given the variability of the method is 25%.

Characterization of perfusion rate and comprehensive process optimization

To characterize rAAV expression in the APEX process, a concerted series of process mapping and range finding studies were performed in laboratory-scale bioreactor cultures. The cell-specific perfusion rate (CSPR) has been demonstrated as a key process parameter in other perfusion-based process, such as monoclonal antibodies,¹² and hence was carefully characterized in the APEX process. The results, shown in Figure 6A, indicate that increasing the CSPR during the production stage increases the cell qP in a linear fashion (the CSPR range was achieved with varying perfusion rate with at infection VCD of $3\text{--}5 \times 10^6$ vc/mL). A plateau was not observed but further perfusion rate was not explored due to the obstacle for its execution at manufacturing scale. In addition, we observed marginally higher full rAAV capsid percentage (Figure 6B), which is desirable for rAAV therapies. The full capsid percentage of Pinnacle PCL is serotype and clone specific, typically ranging from 40% to 80% without optimization.

A process parameter range-finding study was subsequently performed in Ambr250 perfusion bioreactors with one of the hu37 serotype PCL clones (referred as hu37-clone 1) to evaluate six parameters identified to most likely impact rAAV titers (perfusion rate, culture temperature, culture pH, Ad5 MOI, infection VCD and supplemental feed concentration in the perfusion production media). The results of

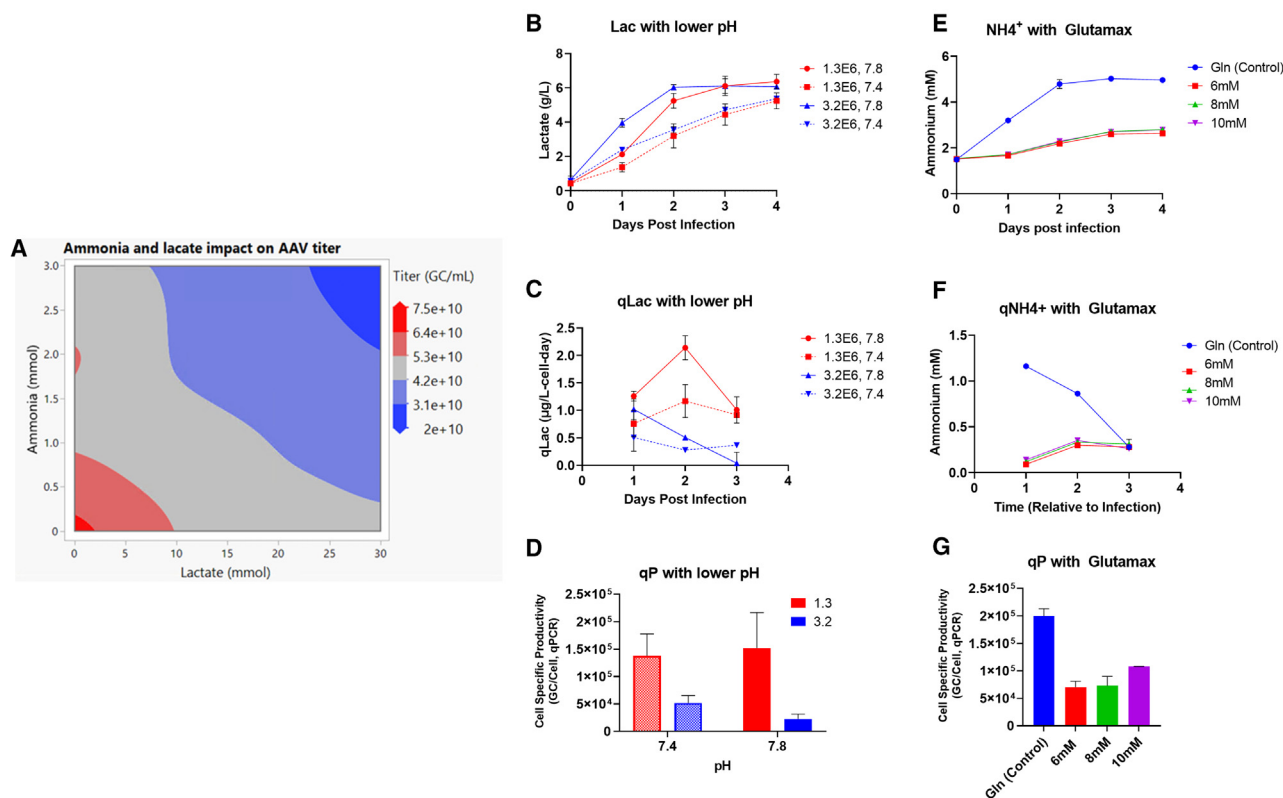


Figure 4. Waste metabolites facilitate the cell density effect

Impact of adding lactate (0–30 mM) and ammonium (0–3 mM) at the time of infection is shown in (A). Lower pH culture from 7.8 to 7.4 in cultures with infection VCD of 1.3×10^6 vc/mL and 3.2×10^6 vc/mL impacted the lactate accumulation (B), lactate cell specific production rate (C), and CSPP (D). We used 6 mM, 8 mM, and 10 mM glutamax instead of 6 mM glutamine and evaluated impact of ammonium accumulation (E), ammonium cell specific production rate (F) and cell qP (G). Data are presented as mean \pm SD.

the range finding study are showed in Figure 6C. Perfusion rate, infection viable cell density (iVCD), and culture temperature all had a relatively strong influence on the resulting rAAV titer results. In contrast, the Ad5 MOI and culture pH had a more muted response on rAAV titers, albeit still a direct relationship. Supplemental feed concentration (5%–15%) was not found significantly correlated to the rAAV titer and hence removed from the model (data now shown). Using JMP statistical software (JMP, Cary, NC), we determined the optimal process parameters for maximizing rAAV titer as follows: perfusion rate of 3.5 VVD (corresponding with a CSPP rate of 500 pL/cell/day), infection VCD of 7×10^6 vc/mL, culture temperature of 35°C, and pH of 7.4. The MOI of Ad5 was selected at 50 viral particle/cell (vp/cell) based on a later study showing similar titer between MOI of 50 and 100 (data not shown) and for Ad5 material conservation consideration. Supplemental feed concentration, not correlated to the titer, was selected at 10%. The optimized APEX process will be referred as APEX P2. The study predicted a maximum AAV titer more than 1.2×10^{12} GC/mL using APEX P2 is possible, which represents an 89% increase from the non-optimized (APEX P1), or a 6-fold titer of batch process. The optimized process parameters capable of supporting the maximized titer were subsequently scaled

and confirmed in a 3L bioreactor culture with ATF-2 and achieved harvest titer of 9.5×10^{11} GC/mL (Figure 6C, far right).

APEX process scalability

The APEX process was successfully scaled-up to a 250L pilot scale bioreactors using three different PCL cells lines, including hu37-clone 1, and hu37-clone 2, that are different monoclonal expressing the same capsid serotype (hu37) and slightly different genes of interest (GOIs) with same disease target, and AAV8-clone 3, which expresses an AAV8 vector with a different GOI for a separate disease target. Figure 7 demonstrated cell density and rAAV titer across the scales of Ambr250, 3L, and 250L when different cell clone and APEX processes are used. The VCD profile and rAAV titer were consistent across scales regardless of the cell clone used with either APEX process. Cell density and rAAV titer from the batch process were also included in Figure 7 to demonstrate the difference between the batch and APEX process. The initial APEX P1 process for hu37-clone 1 demonstrated 3-fold infection VCD and proportional 3-fold rAAV titer relative to the batch control. The optimized APEX P2 process for hu37-clone 2 and AAV8-clone 3 demonstrated approximately 6-fold increase in density and again proportional increase in AAV

Table 1. APEX Process Overview

Day	Key activities	Purpose
0	Initiate production bioreactor control with pH of 7.2, temperature of 37°C. Inoculate the bioreactor with PCL at 0.3×10^6 cells/mL	Production bioreactor starts
3	Start perfusion of growth media at 0.5 VVD	Increase biomass to reach the infection VCD
4	Stop perfusion of growth media and start production media perfusion at 1.5 VVD	Replace the bioreactor with production media to ready the cell culture for production
	Pause perfusion before infection	Avoid losing helper virus through permeate
	Infection of Ad5 helper virus at target MOI	Start AAV production
5	Resume production media perfusion 2 hpi at 3.5 VVD	Eliminate cell density effect
	Set optimal production conditions (pH, temperature)	Facilitate elevated AAV productivity
7	Stop perfusion 48 hpi	AAVs start to release. Avoid losing AAV to permeate
9	Add DNase and hold at least 24 h	Remove host cell DNA to facilitate harvest clarification
10	Harvest (e.g., depth filtration)	Production finish

titer compared with their respective batch controls. Overall scale-up performance showed good scalability across all scales and suggests the APEX process is readily scalable for GMP manufacturing.

DISCUSSION

With the high cost of rAAV-based therapies, improving rAAV manufacturing yields is essential to reduce the cost of production

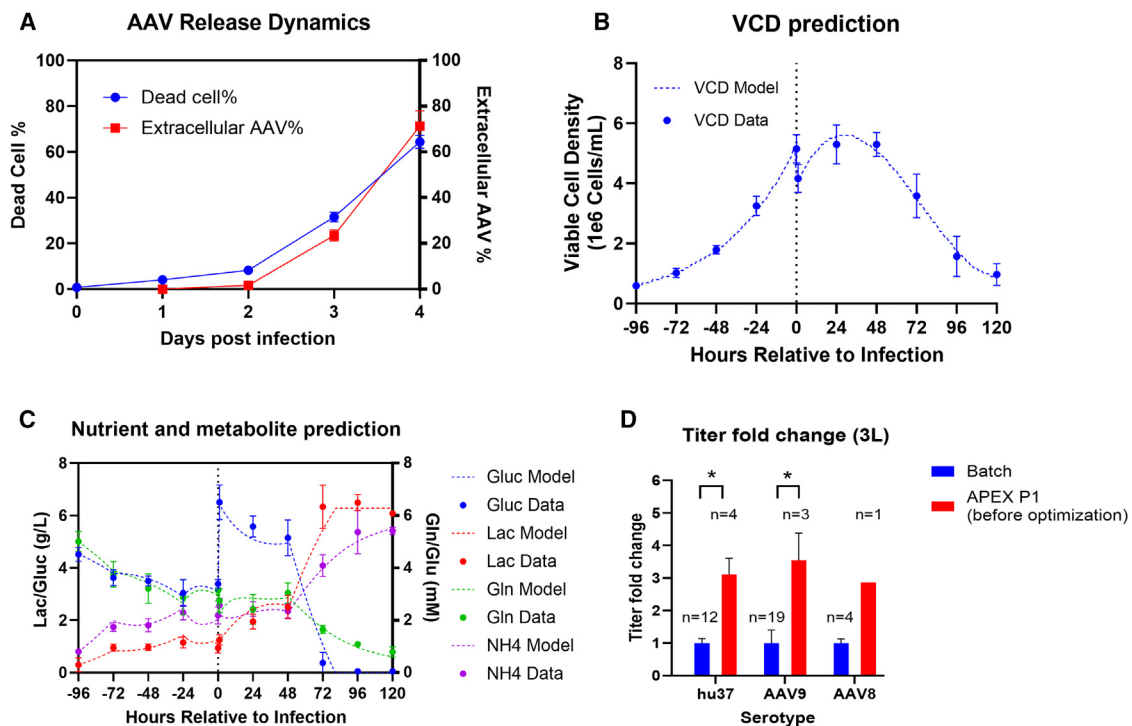


Figure 5. Perfusion process parameters were derived from historical batch process data

(A) The percentage of extracellular rAAV trend with dead cell percentage, suggesting perfusion should stop at 48 hpi. A metabolic model derived from batch process data showed close prediction (dash line) to the experiment data (solid dot) for (B) VCD and (C) nutrient and metabolites prediction with 2.5 VVD perfusion rate. (D) The APEX process demonstrated consistent titer increase from the batch process with three capsid serotypes. Data are presented as mean \pm SD. * $p < 0.05$.

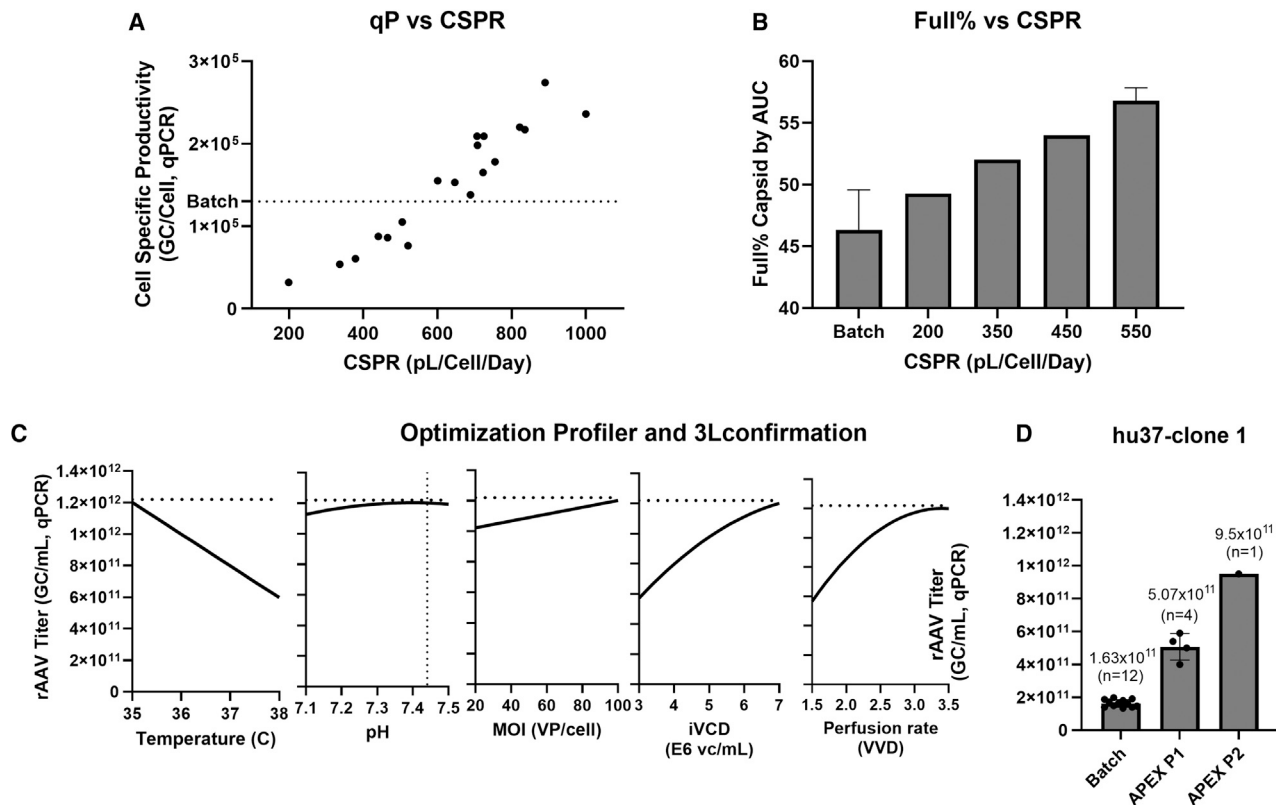


Figure 6. Characterization and optimization of APEX process

(A) Correlation between cell qP and CSPR at infection VCD of $3\text{--}5 \times 10^6$ vc/mL. Cell qP of batch process is shown as the dashed line. (B). Full capsid percentage directly correlates with the CSPR. (C). Optimized APEX process parameters capable of supporting predicted rAAV titer up to 1.2×10^{12} GC/mL. (D) rAAV titer for hu37-clone 1 in batch, APEX P1, and APEX P2 in 3L bioreactors. Data are presented as mean \pm SD.

for these therapies, and expand global patient access. In our initial efforts, we encountered the cell density effect, whereby increasing cell density beyond a threshold resulted in decreased cell specific and volumetric AAV yield (Figure 2). Although too complex to define exactly, it is widely observed in rAAV-producing platforms, including transient transfected HEK-293, baculovirus-infected insect cells, avian cells, and HeLa cells.¹¹ To better understand the cell density effect in the PCL process, we first evaluated whether nutrient deficiency has a contributory role. Among the essential and non-essential amino acids, only glutamine was found to be substantially consumed in batch mode production, which differs from typical batch production of protein biologics. Some amino acids, such as alanine and glutamate, tend to accumulate over the production process, which is commonly observed. As glucose was the other major nutrient consumed throughout the batch production, a daily feed of both glutamine and glucose was tested on cultures infected at slightly higher cell density (1.8×10^6 vc/mL). It was interesting to observe this feeding strategy recovered the glutamine, but not glucose consumption rate compared with the batch control condition. Nonetheless, they did not recover the cell qP to the control level. Although limitations in other nutrients, such as growth factors, vitamins, and trace elements, were not evaluated, these results indicate bulk nutrient

limitation is not the cause of the cell density effect herein. These observations are consistent with previous adenovirus production studies.^{13,14}

Metabolic waste accumulation was also tested as a potential cause for the cell density effect (Figure 3). Lactate and ammonium were fed into cultures of a PCL expressing an hu37 rAAV to ascertain the impact on AAV titer. The rAAV titer decreased in an overlaying and dose-dependent fashion, which is similar to what Shen et al.¹⁵ observed in adenovirus production. With waste metabolite accumulation identified as facilitating the cell density effect, we attempted to attenuate the biochemical pathways to reduce their production. Decreasing extracellular pH, a known approach to reduce glycolysis rates and resulting lactate secretion in our PCLs, was evaluated as a method to improve qP at high cell density. With pH being reduced to 7.4, although lactate accumulation was reduced and qP was somewhat improved in high cell density condition (2.6×10^6 vc/mL), the qP was still significantly lower than the control (VCD of 1.3×10^6 vc/mL). A similar phenomenon was observed for L-alanyl-L-glutamine as an attempt to reduce ammonium production: ammonium accumulation and production were successfully reduced, but the qP was not recovered. Reducing lactate production with lower extracellular pH results in slowing down the

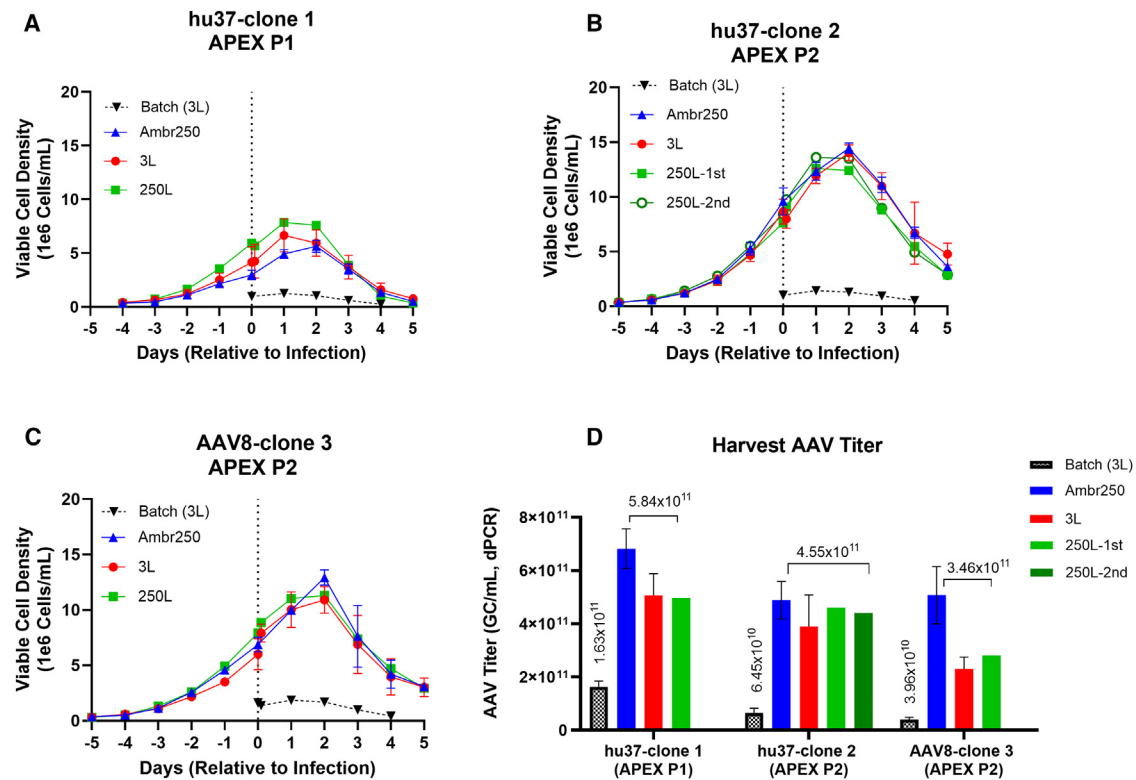


Figure 7. APEX process scalability up to 250L and comparison between batch and APEX processes

(A–C) The VCD for batch process at 3L and APEX processes across AMBR250, 3L, and 250L, respectively, for clone 1 in APEX P1 (A), clone 2 in APEX P2 (B), and clone 3 in APEX P2 (C). The clone 1 and 2 are hu37 serotype PCLs and the clone 3 is an AAV8 serotype PCL. (D) Harvest titer. All titer data was measured by dPCR except that AAV8 in 3L Batch and Ambr250 was measured by qPCR. Data are presented as mean \pm SD. The average titer for batch and APEX processes (across all scales) are labeled above the respective batches.

glycolysis pathway, which is key for cellular energy supply, and thus attenuated rAAV production.^{16,17} Similarly, it is not surprising that slowing down glutaminolysis, which plays a key role in HeLa cell metabolism,¹⁸ resulted in AAV titer reduction as well. This finding has led us to explore physical removal of waste metabolites through perfusion, so that metabolic waste products are kept low in the culture, but not at the expense of the underlying metabolism responsible for their production.

Perfusion has been widely used to improve yields in mammalian cell culture for protein production, such as monoclonal antibodies. Significant process development efforts have been made on media and cell line optimization, scale down model, and control strategy.¹⁹ Recently, a perfusion-based rAAV process has resulted in a 3- to 4-fold rAAV titer increase with HEK-293 transient transfection.⁶ Coronel et al.²⁰ reported up to a 1×10^{12} GC/mL rAAV genome titer with proprietary PCLs ELEVECTA. Due to the terminal nature of the infection-based process of PCLs (Ad5 infection process is cytolytic and kills cells), a continuous production process is not yet possible.

In this work, we have introduced an abbreviated perfusion production process to improve yield, inspired from our own Ad5 infection kinetics

and AAV release (Figure 5A) and literature.¹⁰ We leveraged the cell metabolic rates in batch process to establish a metabolic model to estimate the ideal perfusion rate, which was subsequently confirmed empirically (Figures 5B and 5C). The high accuracy of the prediction suggests that cell metabolic rate was unaltered under high cell density in the APEX process. The only exception was the slower glutamine consumption and ammonium production rate after day 2. The slower metabolism coincided with glucose depletion, which can significantly alter cell cycle and cellular metabolism and lower the glutamine metabolism.^{21–23} We selected an arbitrary factor of one-third to better align the data values with the model. With this first version process, three times cell density was supported while maintaining cell qP, resulting in approximately 3-fold volumetric titer improvement regardless of the capsid serotype (Figure 5D). The significant titer improvements observed with the perfusion of a relatively lean production media as well as the insignificant effect of feed concentration range demonstrated in the range finding study, suggests the cell density effect is driven by waste accumulation, rather than nutrient deficiency. Increased host cell DNA and protein impurities from the APEX process were observed, which is expected due to increased cell mass in the culture and can be reduced to acceptable levels similar to the batch process. Equivalent potency to batch process was also observed (Table S1).

Our initial results examining the CSPR coupled with various infection cell densities showed a linear correlation between CSPR and qP. A less expected but encouraging observation was the full capsid percentage ratio increase with the CSPR (Figure 6B). This could be caused by changes in intracellular processing of AAVs, including capsid production or AAV DNA replication.²⁴

With a more systematic statistical design of experiment approach in the range-finding study (Figure 6), we further increased the volumetric titer by optimizing the targets of six process parameters. In this work, we observed an interaction effect of perfusion rate and cell density on volumetric titer, associated with diminishing improvements within the tested range. Therefore, a combination of infection VCD and perfusion rate was carefully selected to reach an optimum titer. The range finding study predicted a high volumetric titer up to 1.2×10^{12} GC/mL, which was subsequently confirmed in 3L bioreactor at 9.5×10^{11} GC/mL (Figure 6C, far right). Later, this optimized APEX process was successfully scaled up to a 250L bioreactor with comparable volumetric titer (6-fold higher than the batch process) (Figure 7D). To our knowledge, this is the first demonstration of perfusion-based AAV production system using PCL and helper virus beyond bench-scale bioreactors.

The high cost of production for *in vivo* gene therapy treatments remains a huge challenge for the industry. We evaluated the cost of production improvement of the APEX process in comparison to the non-intensified batch process. Although the per-batch cost increased with the APEX process due to fixed capital expenses such as alternating tangential flow (ATF) equipment and operational costs such as additional consumables and media, the 6- to 8-fold AAV titer increase readily outweighed these additional costs and resulted in significant reduction of production cost. The high yield with the APEX process significantly reduces the manufacturing batch requirements to support clinical needs and better supports programs with accelerated timelines and/or high material needs.

To further develop the APEX process and aim for even higher rAAV productivities, additional work will be conducted, including PCL engineering, and process/media improvements to enable an even more efficient cell metabolism. Similar to the experience of monoclonal antibodies, there is typically not a one size fits all strategy when it comes toward leveraging cell/process/media conditions when transitioning from batch or fed-batch processes to intensified ones. Production media optimization to understand impact of individual components on titer and waste generation is particularly important to support lower CSPRs while maintaining rAAV productivity to achieve a cheaper and more robust manufacturing process. With such a pronounced impact on the upstream manufacturing process performance through APEX, the resulting impact toward the downstream process is also profound. We typically observe a proportional increase in process-related impurities such as Ad5, host cell DNA, and host cell proteins that require clearance in the downstream unit operations. Innovations in clarification and downstream processing strategies will continue to be established through the APEX platform to ensure their

successful clearance and conformity with drug substance release criteria.

MATERIALS AND METHODS

Pinnacle PCL generation

Wild-type HeLa S3 cells obtained from European Collection of Authenticated Cell Cultures (Salisbury, UK) were expanded in fetal bovine serum (SAFC, Australia sourced) containing medium, adapted to serum-free suspension conditions, and banked into a research cell bank (RCB) with serum-free media with 10% v/v dimethyl sulfoxide (Origene Biomedical, Austin, TX, USA). This cell bank was thawed and expanded. Then, under puromycin selection pressure, the cells were transfected with triple play plasmid, which contains the AAV vector genome of interest flanked by AAV2 ITRs, AAV replication genes (*Rep*) and capsid genes (*Cap*), puromycin resistance (*PuroR*) gene (for clone selection) and kanamycin resistance (*KanR*) gene (for plasmid manufacture). More than 4,000 transfectant cell pools were isolated and screened for AAV productivity by qPCR in serum-free suspension medium in three rounds of screening. A primary screen was performed in 96-well plates seeded at $1e3$ cells/well, a secondary screen in 24 deep well plates seeded at $2e5$ cells/mL in 3 mL, and a tertiary screen in an ambr15 seeded at $1.5e6$ cells/mL. The top cell lines were cryopreserved into 30-vial RCBs and stored in liquid nitrogen before thawed for experiments. After the parental clone is selected, a limiting dilution step was performed with Solentim Cell Metric CLD (Advanced instrument, Norwood, MA, USA) and followed by the three rounds of screening and banking steps described above. The phenotypical stability of the RCBs, i.e., the AAV titer from production was verified up to 16 weeks of cell expansion in Ambr15, following the procedures detailed in the section Batch production in bioreactors.

Cell expansion

The PCLs were cultured in proprietary growth media and grown in Kuhner shaker incubators (Kuhner, Boston, MA, USA) at 5% CO₂, 37°C, 140 RPM, and 80% humidity. The growth media is a serum free, non-chemically defined nutrition-rich media containing amino acids, sugars, vitamins, and growth factors. VCD was maintained between $0.3e6$ and $5.0e6$ cells/mL during routine passaging. A Vi-Cell XR cell counter (Beckman Coulter, Brea, CA, USA) was used to assess the cell density, viability, and diameter.

Batch production in shake tube and shake flasks

The PCLs were seeded in vented 50-mL shake-tubes (Greiner Bio-One, Monroe, NC, USA), or vented 125-mL Erlenmeyer shake flasks (Corning, Tewksbury, MA, USA) at final culture volumes of 10 mL and 30 mL, respectively. Cultures underwent a media exchange via centrifugation to achieve at least 80% production media, with the remainder being spent growth media from the preceding culture. The production media for batch production is DMEM supplemented with 6 mM glutamine. Production of rAAV was initiated with the addition of wild-type Ad5 at a predetermined MOI. A proprietary supplemental feed was added after infection to support the generation of rAAV. This supplemental feed is a non-chemically defined,

serum-free feed containing amino acids, sugars, and growth factors. Production cultures were incubated in Kuhner shaker incubators at 5% CO₂, 37°C, and 80% humidity for the shake flask and shake tube at 140 RPM and 235 RPM, respectively.

Batch production in bioreactors

For productions at bench scale, the PCLs cultures underwent a media exchange as described previously into Ambr15 vessels (Sartorius, Bohemia, NY, USA), or 3L Mobius bioreactors (Millipore Sigma, Bedford, MA, USA) with the final media conditions being 90% production media with 10% inoculum carry-over in growth media. The working volumes were 13 mL and 2 L, respectively. The target density of the culture was 1.3e6 cells/mL. A proprietary supplemental feed was added after infection to support the generation of rAAV. The bioreactors were operated at controlled temperature, pH, dissolved oxygen, and agitation.

APEX process production

The PCLs were seeded in an Ambr250-HT vessel preassembled with an ATF column (Sartorius, Bohemia, NY, USA), in a 3L Mobius bioreactor attached to an ATF-2 (Repligen, Waltham, MA, USA), or in a 250L HyPerforma bioreactor (Thermo Fisher Scientific, Waltham, MA, USA) attached to an ATF-6 containing the growth media. Two modifications were presented in the growth phase for the process: (a) a blend of growth media and production media was perfused through the reactor 2–3 days prior to infection and followed by a bolus feed at infection, or (b) growth media was perfused from 2 day before infection to 1 day before infection, and production media was perfused 1 day before infection and paused before infection. Production media is formulated with DMEM, 6 mM glutamine, vitamin supplement, and 10% of the proprietary supplement feed, which was also used in the batch production. Production of rAAV at either scale was initiated with the addition of wild-type Ad5 at a predetermined MOI while perfusion was paused for up to 2 h. Perfusion with the production media was reinitiated and maintained for up to 48 hpi. The bioreactors were operated with controlled pH, dissolved oxygen, and temperature.

Cell culture monitoring

Cultures were monitored daily on a Vi-Cell XR cell counter (Beckman Coulter) and FLEX2 Bioanalyzer (Nova Biomedical, Waltham, MA, USA) for cell-health metrics. Samples of culture supernatant was collected after 4–5 days and sterile-filtered before being frozen at –80°C. Samples of culture suspension was collected on required days, treated with 1% Triton X-100 (Thermo Fisher Scientific) for 15 min, then sterile-filtered before being frozen at –80°C. For selected studies, daily supernatant samples were also run on a Rebel analyzer (908 Devices, Boston, MA, USA) for amino acid concentrations in the spent media analysis.

Purification

The harvest material was processed through depth-filtration, anion exchange membrane, tangential flow filtration, and affinity chromatography with retains pulled at each unit operation. Bench-scale ma-

terial went through an abbreviated purification scheme depending on the experiment.

Genome titer by qPCR and dPCR

For both methods, samples were initially treated with salt active nuclease (SAN, ArcticZymes, Tromsø, Norway) to remove non-encapsidated DNA. The rAAV samples were then treated with Proteinase K (Thermo Fisher Scientific) to inactivate SAN and digest the viral capsid.

For qPCR method, the samples were then mixed with a primer sequence targeting a region of the rAAV genome in the rAAV therapeutic products. The qPCR was performed on an Applied Biosystems Flex 6 or 7 instrument (Thermo Fisher Scientific) and the amount of DNA was quantified based on the threshold cycle (Ct) comparing with a linearized DNA standard using the QuantStudio 6/7 software.

For digital PCR (dPCR) method, the samples were then diluted to a target concentration in TE buffer + 0.1% Pluronic buffer. Samples were mixed with 4X dPCR Master Mix and 10X GOI primers/probe targeting the sequence of interest. This mixture was then transferred to the QIAcuity nanoplates and placed in the QIAcuity (Qiagen, Germantown, MD Ct) for sample partitioning, PCR amplification, and imaging. As the template is distributed randomly, Poisson statistics were used to calculate the amount of target DNA per positive partition.

Host cell DNA and Ad5 DNA by qPCR

The rAAV samples were treated with Proteinase K (Thermo Fisher Scientific) to digest the viral capsid. Treated samples were then diluted and subjected to qPCR using a primers/probe set that targets Alu repeat sequences for host cell DNA, and E2A gene for residual Ad5 DNA. The qPCR was performed on an Applied Biosystems Flex 6 or 7 instrument (Thermo Fisher Scientific) and the amount of DNA was quantified based on the Ct comparing to a linearized DNA standard using the QuantStudio 6/7 software.

Host cell protein quantification by ELISA

The host cell protein was determined by an ELISA method with Cygnus HeLa HCP ELISA kit (Cygnus Technology, Leland, NC, USA). Samples containing HeLa cell proteins were reacted in microtiter strips pre-coated with an affinity purified capture antibody. A second horseradish peroxidase-labeled anti-HeLa HCP antibody was reacted simultaneously, forming a sandwich complex of solid phase antibody-HeLa HCP enzyme labeled antibody. The microtiter strips were then washed to remove any unbound reactants. After the washes, the substrate tetramethylbenzidine was applied to elicit a color change reaction. The intensity of the color generated was directly proportional to the amount of HeLa HCP in the sample. The concentration was determined based on extrapolation against a standard curve.

Relative potency by protein expression

The relative potency was determined by rAAV protein expression in C2C12 cells by an ELISA method (key reagents from Meso Scale Diagnostics, Rockville, MD, USA). Prior to testing, rAAV was purified

by affinity chromatography. C2C12 mouse myoblast cells (Sigma-Aldrich, St. Louis, MO, USA) were cultured, plated, and differentiated in a gelatin coated 96-well plate. The cells were then infected with purified AAV at target MOIs and cultured for additional 4 days, and then harvested and lysed. Then the cell lysate was transferred to a 96-well plate coated with MANDYS106 antibodies (Millipore Sigma, Bedford, MA, USA), and unlabeled detection antibodies DysB (Leica Biosystems, Deer Park, IL, USA) followed by anti-species antibodies conjugated with electro-chemiluminescent label (Polyclonal Goat Anti-Mouse Sulfo-Tag Labeled Antibody from Meso Scale Diagnostics) over the course of three incubation periods. Then the plate was evaluated with MESO QuickPlex ESQ 120MM system (Meso Scale Diagnostics) and the readout was normalized to a reference standard.

Empty, intermediate, and full rAAV quantitation by SV-AUC

The percentage of empty particles, intermediate particles and full rAAV particles were quantitated by sedimentation velocity analytical ultracentrifugation (SV-AUC Proteomelab XL-A/XL-I, Beckman Coulter) using absorption optics at 230 nm. Prior to testing, the material was purified by affinity chromatography. The rate of sedimentation of empty, intermediate, and full rAAV particles was measured when subjected to high centrifugal force. The sedimentation coefficient distribution for each species was quantitated by area under peak.

Metabolic model

A metabolic model was developed to predict metabolite profiles (glucose, lactate, glutamine, and ammonium) of the APEX production system to determine multiple process parameters such as perfusion rate. The Euler method with a time interval of 1 h was used to solve each differential equation. This model includes a total of 20 inputs, including the initial VCD, initial metabolites (glucose, lactate, glutamine and ammonium), cell growth rate, metabolite (glucose, lactate, glutamine and ammonium) production or consumption rates for growth and production (derived from batch process data), glucose and glutamine concentration in the growth and production media, glutamine degradation rate, and perfusion rate.

Equations used for metabolite production and consumption are below:²⁵

$$\mu = \frac{1}{C_v} \left(\frac{dC_v}{dt} \right)$$

$$q_{Glc} = \frac{1}{C_v} \left(D(Glc_{medium} - Glc) - \frac{dGlc}{dt} \right)$$

$$q_{Lac} = \frac{1}{C_v} \left(D(Lac) + \frac{dLac}{dt} \right)$$

$$q_{Gln} = \frac{1}{C_v} \left(D(Gln_{medium} - Gln) - \frac{dGln}{dt} - r_{degr}Gln \right)$$

$$q_{Amm} = \frac{1}{C_v} \left(D(Amm - Amm_{medium}) + \frac{dAmm}{dt} - r_{degr}Amm \right),$$

where $q_{glc}/q_{lac}/q_{gln}/q_{amm}$ are the consumption rate glucose, lactate, glutamine, and ammonium, respectively; μ is the cell growth rate; D is the perfusion rate; C_v is the VCD; and r_{degr} is the degradation rate of glutamine.

The assumption of metabolic model included the following: an exponential regression was used for the growth-stage VCD, and a cubic regression was used for the production-stage VCD. A 25% change in VCD and metabolites was accounted for due to changes in reactor working volume with supplemental feed. The glutamine generation and ammonium production rates after day 2 post infection through production end were decreased to one-third of their day 0 through day 2 production values. The degradation rate of glutamine at 37°C has been reported as between 7% and 10% of the glutamine present per day.^{26,27} A value of 8% was used for the model.

Design of experiments for parameter range finding

The parameter range finding study investigated impact on the rAAV titer from six parameters, including temperature, pH, perfusion rate, infection VCD, MOI, and supplemental feed concentration. The design was created with JMP software, and was a central composite design, with 2 blocks of 24 Ambr250 reactors, aiming to evaluate all main effects, secondary interactions, and square terms of all the parameters. The final model was selected based on the minimum Bayesian information criterion. As a result, supplemental feed concentration was not included in the model. The parameters set with maximized titer was selected for the optimized APEX process.

Calculations

The equation for CSPR is shown below and expressed by dividing the VVD rate by the cell density (viable cells per milliliter) at the time of Ad5 infection and converting units to pL/cell/day. CSPR is independent of exact vessel volume as the term of “vessel volume” cancels out on both sides of the equation. For example, one of the data points in Figure 6B that shows VVD of 3.5 corresponds with a CSPR of 500 pL/cell/day when the infection VCD is 7e6 cells/mL.

$$CSPR = \frac{VVD \times Vessel\ volume}{Cell\ density \times Vessel\ volume}$$

Cell qP was calculated by dividing the harvest rAAV yield by the cell density at the time of Ad5 infection.

The cell-specific consumption rate of glucose and glutamine and cell-specific consumption rate of lactate and ammonium, were calculated by dividing the difference of the value between two consecutive daily samples by average VCD of the 2 days, then divided by the time interval (1 day).

DATA AND CODE AVAILABILITY

Ultragenyx Pharmaceuticals is unable to provide materials, additional datasets, or protocols.

SUPPLEMENTAL INFORMATION

Supplemental information can be found online at <https://doi.org/10.1016/j.omtm.2024.101266>.

ACKNOWLEDGMENTS

The authors are grateful for the Downstream Development, Analytical Development, and Pilot Plant teams in the Global CMC Development Department, and Producer Cell Line and Gene Therapy Research Department at Ultragenyx Pharmaceuticals for their support. This work was funded by Ultragenyx Pharmaceuticals.

AUTHOR CONTRIBUTIONS

Conceptualization: W.X., C.F., J.P., and J.W.; data curation, W.X. and C.F.; formal analysis: W.X. and C.F.; investigation: W.X., C.F., N.A., and S.S.; methodology: W.X. and C.F.; project administration: W.X., J.P., and P.H.; resources and supervision: J.W.; visualization: W.X., C.F., and S.S.; manuscript draft: W.X., C.F., S.S., P.H., and J.W.; manuscript review and editing: all authors.

DECLARATION OF INTERESTS

This work was funded by Ultragenyx Pharmaceuticals. All authors were employed by Ultragenyx Pharmaceuticals when the experiments were executed. Several authors are shareholders of Ultragenyx Pharmaceuticals. The work is related to patent WO2023172491A1 - Modified batch aav production systems and methods.

REFERENCES

- Flotte, T.R., and Carter, B.J. (1998). Adeno-associated virus vectors for gene therapy of cystic fibrosis. *Methods Enzymol.* 292, 717–732. [https://doi.org/10.1016/S0076-6879\(98\)92055-9](https://doi.org/10.1016/S0076-6879(98)92055-9).
- Sha, S., Maloney, A.J., Katsikis, G., Nguyen, T.N.T., Neufeld, C., Wolfrum, J., Barone, P.W., Springs, S.L., Manalis, S.R., Sinskey, A.J., and Braatz, R.D. (2021). Cellular pathways of recombinant adeno-associated virus production for gene therapy. *Biotechnol. Adv.* 49, 107764. <https://doi.org/10.1016/j.biotechadv.2021.107764>.
- Wang, D., Tai, P.W.L., and Gao, G. (2019). Adeno-associated virus vector as a platform for gene therapy delivery. *Nat. Rev. Drug Discov.* 18, 358–378. <https://doi.org/10.1038/s41573-019-0012-9>.
- Monahan, P.E., and Samulski, R.J. (2000). Adeno-associated virus vectors for gene therapy: More pros than cons? *Mol. Med. Today* 6, 433–440. [https://doi.org/10.1016/S1357-4310\(00\)01810-4](https://doi.org/10.1016/S1357-4310(00)01810-4).
- Xiao, X., Li, J., and Samulski, R.J. (1998). Production of High-Titer Recombinant Adeno-Associated Virus Vectors in the Absence of Helper Adenovirus. *J. Virol.* 72, 2224–2232. <https://doi.org/10.1128/jvi.72.3.2224-2232.1998>.
- Mendes, J.P., Fernandes, B., Pineda, E., Kudugunti, S., Bransby, M., Gantier, R., Peixoto, C., Alves, P.M., Roldão, A., and Silva, R.J.S. (2022). AAV process intensification by perfusion bioreaction and integrated clarification. *Front. Bioeng. Biotechnol.* 10, 1020174. <https://doi.org/10.3389/fbioe.2022.1020174>.
- Clark, K.R., Voulgaropoulou, F., Fraley, D.M., and Johnson, P.R. (1995). Cell lines for the production of recombinant adeno-associated virus. *Hum. Gene Ther.* 6, 1329–1341.
- Tatalick, L.M., Gerard, C.J., Takeya, R., Price, D.N., Thorne, B.A., Wyatt, L.M., and Anklesaria, P. (2005). Safety characterization of HeLa-based cell substrates used in the manufacture of a recombinant adeno-associated virus-HIV vaccine. *Vaccine* 23, 2628–2638. <https://doi.org/10.1016/j.vaccine.2004.11.027>.
- Thorne, B.A., Takeya, R.K., and Peluso, R.W. (2009). Manufacturing recombinant adeno-associated viral vectors from producer cell clones. *Hum. Gene Ther.* 20, 707–714. <https://doi.org/10.1089/hum.2009.070>.
- Crisostomo, L., Soriano, A.M., Mendez, M., Graves, D., and Pelka, P. (2019). Temporal dynamics of adenovirus 5 gene expression in normal human cells (PLoS ONE (2019) 14:1 (e0211192) DOI: 10.1371/journal.pone.0211192). *PLoS One* 14, 1–18. <https://doi.org/10.1371/journal.pone.0211192>.
- Lavado-García, J., Pérez-Rubio, P., Cervera, L., and Gòdia, F. (2022). The cell density effect in animal cell-based bioprocessing: Questions, insights and perspectives. *Biotechnol. Adv.* 60, 108017. <https://doi.org/10.1016/j.biotechadv.2022.108017>.
- Maria, S., Bonneau, L., Fould, B., Ferry, G., Boutin, J.A., Cabanne, C., Santarelli, X., and Joucla, G. (2023). Perfusion process for CHO cell producing monoclonal antibody: Comparison of methods to determine optimum cell specific perfusion rate. *Biochem. Eng. J.* 191, 108779. <https://doi.org/10.1016/j.bej.2022.108779>.
- Yuk, I.H.Y., Olsen, M.M., Geyer, S., and Forestell, S.P. (2004). Perfusion cultures of human tumor cells: A scalable production platform for oncolytic adenoviral vectors. *Biotechnol. Bioeng.* 86, 637–642. <https://doi.org/10.1002/bit.20158>.
- Maranga, L., Aunins, J.G., and Zhou, W. (2005). Characterization of Changes in PER.C6™ cellular metabolism during growth and propagation of a replication-deficient adenovirus vector. *Biotechnol. Bioeng.* 90, 645–655. <https://doi.org/10.1002/bit.20455>.
- Shen, C.F., Voyer, R., Tom, R., and Kamen, A. (2010). Reassessing culture media and critical metabolites that affect adenovirus production. *Biotechnol. Prog.* 26, 200–207. <https://doi.org/10.1002/btpr.286>.
- Henry, O., Perrier, M., and Kamen, A. (2005). Metabolic flux analysis of HEK-293 cells in perfusion cultures for the production of adenoviral vectors. *Metab. Eng.* 7, 467–476. <https://doi.org/10.1016/j.jymben.2005.08.002>.
- Petiot, E., Cuperlovic-Culf, M., Shen, C.F., and Kamen, A. (2015). Influence of HEK293 metabolism on the production of viral vectors and vaccine. *Vaccine* 33, 5974–5981. <https://doi.org/10.1016/j.vaccine.2015.05.097>.
- Kimura, T., Ferran, B., Tsukahara, Y., Shang, Q., Desai, S., Fedoco, A., Pimentel, D.R., Luptak, I., Adachi, T., Ido, Y., et al. (2019). Production of adeno-associated virus vectors for *in vitro* and *in vivo* applications. *Sci. Rep.* 9, 13601–13613. <https://doi.org/10.1038/s41598-019-49624-w>.
- Bielsler, J.M., Wolf, M., Souquet, J., Broly, H., and Morbidelli, M. (2018). Perfusion mammalian cell culture for recombinant protein manufacturing – A critical review. *Biotechnol. Adv.* 36, 1328–1340. <https://doi.org/10.1016/j.biotechadv.2018.04.011>.
- Coronel, J., Patil, A., Al-Dali, A., Braß, T., Faust, N., and Wissing, S. (2021). Efficient production of rAAV in a perfusion bioreactor using an ELEVECTA® stable producer cell line. *Genet. Eng. Biotechnol. News* 41, S23. <https://doi.org/10.1089/gen.41.S2.07>.
- Colombo, S.L., Palacios-Callender, M., Frakich, N., Carcamo, S., Kovacs, I., Tudzarova, S., and Moncada, S. (2011). Molecular basis for the differential use of glucose and glutamine in cell proliferation as revealed by synchronized HeLa cells. *Proc. Natl. Acad. Sci. USA* 108, 21069–21074. <https://doi.org/10.1073/pnas.1117500108>.
- Shiratori, R., Furuichi, K., Yamaguchi, M., Miyazaki, N., Aoki, H., Chibana, H., Ito, K., and Aoki, S. (2019). Glycolytic suppression dramatically changes the intracellular metabolic profile of multiple cancer cell lines in a mitochondrial metabolism-dependent manner. *Sci. Rep.* 9, 18699–18715. <https://doi.org/10.1038/s41598-019-55296-3>.
- Chioldi, I., Picco, G., Martino, C., and Mondello, C. (2019). Cellular response to glutamine and/or glucose deprivation in *in vitro* transformed human fibroblasts. *Oncol. Rep.* 41, 3555–3564. <https://doi.org/10.3892/or.2019.7125>.
- Nguyen, T.N.T., Sha, S., Hong, M.S., Maloney, A.J., Barone, P.W., Neufeld, C., Wolfrum, J., Springs, S.L., Sinskey, A.J., and Braatz, R.D. (2021). Mechanistic model for production of recombinant adeno-associated virus via triple transfection of

- HEK293 cells. *Mol. Ther. Methods Clin. Dev.* 21, 642–655. <https://doi.org/10.1016/j.omtm.2021.04.006>.
25. Jagušić, M., Forčić, D., Brgles, M., Kutle, L., Šantak, M., Jergović, M., Kotarski, L., Bendelja, K., and Halassy, B. (2016). Stability of Minimum Essential Medium functionality despite l-glutamine decomposition. *Cytotechnology* 68, 1171–1183. <https://doi.org/10.1007/s10616-015-9875-8>.
26. Tritsch, G.L., and Moore, G.E. (1962). Spontaneous decomposition of glutamine in cell culture media. *Exp. Cell Res.* 28, 360–364. [https://doi.org/10.1016/0014-4827\(62\)90290-2](https://doi.org/10.1016/0014-4827(62)90290-2).
27. Clincke, M.F., Mölleryd, C., Zhang, Y., Lindskog, E., Walsh, K., and Chotteau, V. (2013). Very high density of CHO cells in perfusion by ATF or TFF in WAVE bioreactor™: Part I: Effect of the cell density on the process. *Biotechnol. Prog.* 29, 754–767. <https://doi.org/10.1002/btpr.1704>.